UC Irvine
UC Irvine Previously Published Works

Title
Wavelengths for port wine stain laser treatment: influence of vessel radius and skin anatomy

Permalink
https://escholarship.org/uc/item/1nt4b1wj

Journal
Physics in Medicine and Biology, 42(1)

ISSN
0031-9155

Authors
van Gemert, Martin JC
Smithies, Derek J
Verkruysse, Wim
et al.

Publication Date
1997

DOI
10.1088/0031-9155/42/1/002

Peer reviewed

Wavelengths for port wine stain laser treatment: influence of vessel radius and skin anatomy

Martin J C van Gemert†‡§, Derek J Smithies†, Wim Verkruysse‡,
Thomas E Milner† and J Stuart Nelson†

† Beckman Laser Institute and Medical Clinic, Irvine, CA, USA
‡ Laser Centre, Academic Medical Centre, Amsterdam, The Netherlands

Abstract. Recent Monte Carlo computations in realistic port wine stain (PWS) models containing numerous uniformly distributed vessels suggest equal depth of vascular injury at wavelengths of 577 and 585 nm. This finding contradicts clinical experience and previous theory. From a skin model containing normal and PWS vessels in separate dermal layers, we estimate analytically the average volumetric heat production in the deepest targeted PWS vessel. The fluence rate distribution is approximated by Beer's law, which depends upon the tissue's effective attenuation coefficient, and includes a homogeneous fractional volumetric blood concentration corrected for finite-size blood vessels. The model predicts 585–587 nm wavelengths are optimal in adult PWSs containing at least one layer of small-radius blood vessels. In superficial PWSs, typically in young children with small-radius vessels, 577–580 nm wavelengths are optimal. Wavelength-independent results similar to those from Monte Carlo models are valid in single-layered PWSs of large-radius vessels. In conclusion, the volumetric heat production in the deepest targeted PWS blood vessel can be maximized on an individual patient basis. However, absorption of 585–587 nm wavelengths is sufficiently high in superficial lesions, so we hypothesize that these wavelengths may be considered adequate for the treatment of any PWS.

1. Introduction

The ideal laser wavelength to achieve selective photothermolysis of port wine stain (PWS) blood vessels has still to be identified beyond any doubt, despite considerable previous research efforts (e.g. Anderson and Parrish 1981, Tan *et al* 1989a, 1990, van Gemert *et al* 1995a.)

Selective photothermolysis assumes 577 nm is the optimum wavelength for irreversible injury of isolated blood vessels, as oxyhaemoglobin absorption is maximized relative to that of epidermal melanin and dermal collagen (Anderson and Parrish 1981, van Gemert and Hulsbergen Henning 1981). Shifting the wavelength to 585 nm was shown by Tan *et al* (1990) to increase the dermal depth at which irreversible vascular injury in PWS occurred. In addition, these authors found that adult patients who had incomplete clearance of their PWS at 577 nm, successfully responded to 585 nm irradiation. Theoretical studies have sought to explain these observations.

Pickering and van Gemert (1991) hypothesized that red blood cells (RBCs) contained in superficial dermal vessels act as an absorbing 'optical shield' for scattered photons;

§ Correspondence: J Stuart Nelson, Beckman Laser Institute and Medical Clinic, 1002 Health Sciences Road East, Irvine, CA 92612, USA. E-mail address: snelson@bli.uci.edu

this reduces the fluence rate in deeper skin regions. Thus, when the laser wavelength is increased from 577 to 585 nm, blood absorption is reduced by a factor of two, so more light reaches the deeper vessels. This concept was evaluated further by Verkruysse *et al* (1993), van Gemert *et al* (1995b), and Kienle and Hibst (1995), approximating discrete vessels by a homogeneous fractional volumetric blood concentration (*homogeneous model*), resulting in predicted wavelength-dependent depth of vascular injury similar to that observed in clinical experiments (Tan *et al* 1989a, 1990).

In contrast, results from Monte Carlo models containing numerous uniformly distributed PWS blood vessels within the targeted region (*discrete vessel model*) show virtually identical vascular volumetric heat production at 577 and 585 nm, and do not indicate which wavelength is optimal for PWS treatment (Smithies and Butler 1995, Lucassen *et al* 1996). An explanation for the difference between the models is that RBCs at the centre of the lumen contribute less to light attenuation than those adjacent to the vessel wall, particularly if the radius is much larger than the blood absorption length (Svaasand *et al* 1995, Verkruysse *et al* 1997). Therefore, as blood absorption increases, the number of RBCs per vessel that contribute to heat production decreases. The homogeneous model does not include this effect of discrete vessels because all RBCs at a given dermal depth contribute equally to light absorption. Thus, light attenuation is higher in the homogeneous than discrete vessel model. A correction factor should be used to reduce the number of RBCs in the homogeneous model so the fluence rate distribution obtained is equal to that from the discrete vessel model (Svaasand *et al* 1995, Verkruysse *et al* 1997). However, although use of the correction factor explains the different results from the two models, it does not explain the wavelength-dependent effects observed in PWS patients by Tan *et al* (1990).

The purpose of this paper is, first, to identify two causes for the conflicting results observed between the models and clinical experience, and, second, to use this information to reexamine the importance of wavelength for PWS laser treatment, A new, compound, anatomical skin model is proposed, which consists of two homogeneous dermal layers, each of which can contain either PWS vessels or normal-sized capillaries, and which includes the correction factor for finite blood vessels. In four different models of PWS anatomies, volumetric heat production in the deepest targeted PWS vessel is analytically estimated for wavelengths between 575 and 600 nm.

2. Model

The skin model chosen incorporates histological data from Barsky *et al* (1980) and Tan *et al* (1990). The former show considerable variability in PWS vessel size, so radii chosen reflect the range reported. The latter provide histological pictures, suggesting a multi-layered dermal model is required.

The PWS skin model used in this work (figure 1) consists of an epidermis and dermis; the latter is composed of two layers, of thicknesses z_1 and z_2 (mm), and includes a targeted blood vessel of radius R_3 (mm), located at $z_3 = z_1 + z_2$ (mm) from the epidermal–dermal interface. The dermal layers contain blood vessels of radii R_1 and R_2 (mm), constituting fractional dermal volumetric blood concentrations of F_1 and F_2, reduced by factors C_1 and C_2 to correct the fluence rate distribution for the effect of non-zero blood vessel radii. Correction factor C (figure 2) is equal to the vessel's cross sectional average relative fluence rate and depends on the non-dimensional product of vessel radius R and blood absorption coefficient $\mu_{ab}(\lambda)$ (mm^{-1}) at wavelength λ (Verkruysse *et al* 1997).
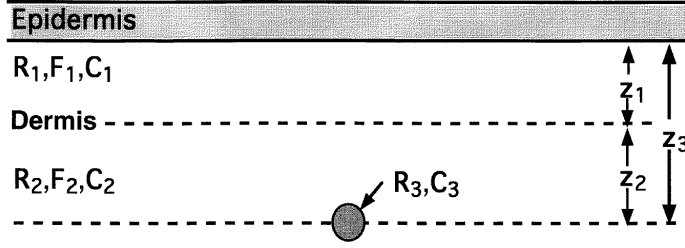
Figure 1. The anatomy of PWS skin used. Parameters R_1, F_1 and C_1 for the upper dermal layer denote, respectively, the layer's average blood vessel radius, fractional volumetric blood concentration, and correction factor to account for non-zero vessel radii. Similarly, R_2, F_2 and C_2 refer to the deeper dermal layer, and R_3 and C_3 to the deepest targeted PWS blood vessel.
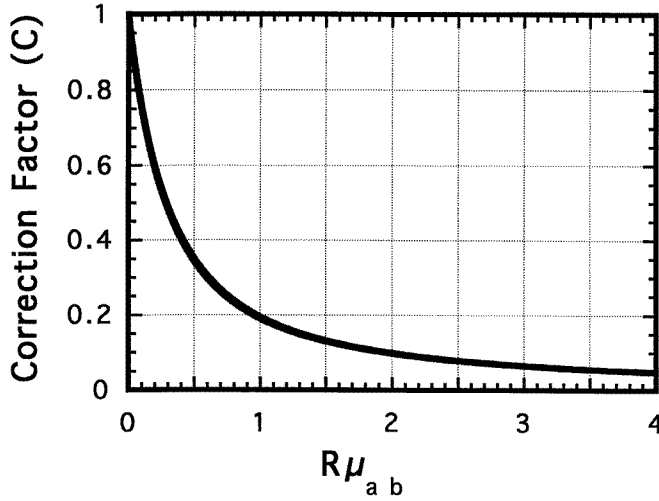

Figure 2. The correction factor $C(R\mu_{ab})$ represents the vessel's cross sectional average relative fluence rate. It is used to reduce the dermal fractional volumetric blood concentration in the homogeneous model so that fluence rate distributions are equal to those obtained from the discrete vessel model (from Verkruysse *et al* 1997).

The light fluence rate at dermal depth z_3, $\phi(z_3)$ (W mm^{-2}), is approximated as

$$\phi(z_3) = EA_e \exp(-z_1\mu_{\text{eff1}}) \exp(-z_2\mu_{\text{eff2}}) \tag{1}$$

where E, A_e, μ_{eff1} and μ_{eff2} denote, respectively, laser irradiance (W mm^{-2}), epidermal attenuation, and effective attenuation coefficients (mm^{-1}) of layers 1 and 2. Equation (1) follows from diffusion theory (see e.g. Star 1995, p 161) using an infinitely wide laser beam. Parameters μ_{eff1} and μ_{eff2} are defined as

$$\mu_{\text{eff}j} = \sqrt{3\langle\mu_{aj}\rangle[\langle\mu_{aj}\rangle + \langle\mu'_{sj}\rangle]} \qquad j = 1, 2 \tag{2a}$$

where $\langle\mu_{aj}\rangle$ and $\langle\mu'_{sj}\rangle$ denote the layer's average absorption and reduced scattering coefficients, respectively. These are approximated as

$$\langle\mu_{aj}(\lambda)\rangle \approx F_j C_j \mu_{ab}(\lambda) \qquad j = 1, 2 \tag{2b}$$

$$\langle\mu'_{sj}\rangle \approx \mu'_{sd} \approx 1.47 \text{ mm}^{-1} \qquad j = 1, 2 \tag{2c}$$

Table 1. The four models evaluated in this paper, representative of four different PWS anatomies. The anatomy is shown schematically in figure 1; the cross sectional average volumetric heat production Q_3 of the deepest targeted vessel of radius R_3 is expressed in equation (3). For each model, the calculated values of Q_3 normalized to $EA_e = 1$ (W mm^{-2}), are given, respectively, in figures 3(A), 3(B), 3(C) and 3(D).

Model	R_1 (μm)	z_1 (mm)	F_1	R_2 (μm)	z_2 (mm)	F_2	R_3 (μm)	Comment
1	50	0.3	0.15	2	0–1	0.02	50	Figure 2 of Tan *et al* (1990)
2	12.5	0.15	0.05	2	0–0.5	0.02	12.5	Light PWS in child
3	2	0–1	0.02	0	0	0	50	Incompletely treated PWS
4	0–100	0.75	0.05	0	0	0	0–100	Single layered PWS, $R_1 = R_3$

where μ'_{sd} denotes the reduced scattering coefficient of normal dermis; the value used is from the article by Kienle and Hibst (1995).

We have neglected small wavelength-independent contributions of light absorption of normal dermal tissue in (2*b*), and light scattering of blood in (2*c*), as well as a small wavelength-dependent effect, caused by blood absorption, which reduces the fluence rate distribution close to the targeted vessel. Most importantly, however, the fluence rate near the air–tissue interface exceeds the irradiance by a factor between one and five (see e.g. Star 1995, p 194) depending upon whether the ratio of the tissue's absorption and reduced scattering coefficients is large or very small, respectively. Within the 577–600 nm wavelength band considered, blood absorption decreases substantially (by a factor of about 20) and, from (2*b*), the average dermal absorption coefficient decreases proportionately. This produces an increase in fluence rate at the tissue–air boundary when the wavelength changes from 577 to 600 nm. The present analysis neglects this effect as A_e in (1) is taken to be wavelength independent. The model may therefore underestimate the extent of wavelength-dependent effects occurring during laser treatment.

The volumetric cross sectional average heat production, $Q_3(z_3)$ (W mm^{-3}), in the diffusely irradiated deepest targeted PWS vessel, of radius R_3, located at dermal depth $z_3 = z_1 + z_2$, is

$$Q_3(z_3) = \mu_{ab}C_3\phi(z_3) \tag{3}$$

where C_3 is the correction factor for this vessel. Following Kienle and Hibst (1995), the criterion for irreversible vascular injury was assumed to depend on the vessel's cross sectional average volumetric heat production, which is proportional to the product of blood absorption, μ_{ab}, and cross sectional average fluence rate, $C_3\phi(z_3)$.

Four different models of PWS anatomies, specified in table 1, were considered. The first model is derived from the histological picture of an adult PWS published in figure 2 of Tan *et al* (1990). It shows a superficial plexus ($z_1 \approx 0.3$ mm) containing large-radius vessels ($R_1 \approx 50$ μm), constituting a substantial fractional volumetric blood concentration ($C_1 \approx 0.15$), above a semi-normal dermal layer ($z_2 \approx 0.8$ mm, assuming $R_2 = 2$ μm and $C_2 = 0.02$). In the model, z_2 was varied between 0 and 1 mm.

The second model represents a PWS in a young child ($z_3 < 0.65$ mm; see skin thickness as a function of age, Tan *et al* 1982), using a superficial plexus ($z_1 = 0.15$ mm) of small-diameter vessels ($R_1 = 12.5$ μm) and small fractional volumetric blood concentration ($C_1 = 0.05$). We assume this anatomy represents a light-coloured PWS.

The third model represents an incompletely treated PWS, where the 'deepest targeted vessel' is the shallowest vessel of the residual lesion. Here, the second dermal layer is not

explicitly incorporated; this requires setting $z_2 = 0$ in (1). We tacitly assume injury of the targeted vessel represents injury of the residual lesion.

The fourth model corresponds to the single-layered PWS used in previous computations (Pickering and van Gemert 1991, Verkruysse *et al* 1993, van Gemert *et al* 1995b, Kienle and Hibst 1995, Smithies and Butler 1995, Lucassen *et al* 1996).

3. Results

3.1. The first PWS model

In figure 3(A), the cross sectional average volumetric heat production in the deepest targeted PWS vessel, Q_3, normalized to $EA_e = 1$ (W mm^{-2}), is shown for an adult PWS model, where thickness (z_2) of the second layer is varied between 0 and 1 mm in steps of 0.2 mm. The results predict that a wavelength-specific maximum in Q_3 occurs at 586–591 nm for $z_2 > 0.2$ mm.

Tan *et al* (1990) evaluated in a histologic study the depth of vascular injury in six adult facial PWS patients in response to 6–7 J cm^{-2} radiant exposure, 0.36 ms pulse duration, 3 mm spot size diameter, 577 and 585 nm wavelengths laser irradiation. At 577 nm, the maximum dermal depth of vascular injury was observed between 0.65 and 0.8 mm (average 0.72 ± 0.02 mm) and at 585 nm between 1.0 and 1.3 mm (average 1.16 ± 0.06 mm).

The model predicts identical values of Q_3 at 577 and 585 nm, for dermal depths of 0.95 mm and 1.16 mm, respectively, virtually independent of the value used for the reduced dermal scattering coefficient μ'_{sd}. We hypothesize the difference between model prediction and clinical outcome at 577 nm (0.95 versus 0.72 mm), assuming 1.16 mm is the depth of vascular injury at 585 nm, is due to the increase in fluence rate occurring at wavelengths longer than 577 nm, a mechanism neglected in equation (1).

3.2. The second PWS model

In figure 3(B), the results are shown for a light-coloured PWS in a young child, varying the thickness of the second semi-normal dermal layer (z_2) between 0 and 0.5 mm in steps of 0.1 mm. The model predicts that the maximum occurring in Q_3 remains virtually at 577 nm, except for larger values of z_2 where it is between 577 and 583 nm wavelengths.

3.3. The third PWS model

In figure 3(C), predictions for an incompletely treated PWS model are shown using a semi-normal dermis, varying its thickness z_1 between 0 and 1 mm in steps of 0.2 mm. The results suggest that Q_3 attains a maximum at wavelengths between 584 and 588 nm at dermal depths greater than 0.2 mm. Recalling that the model tends to underestimate wavelength-dependent effects during laser treatment, this explains observations in clinical experiments (Tan *et al* 1990) that adult patients who had incomplete clearance of their PWS at 577 nm successfully responded to 585 nm irradiation.

3.4. The fourth PWS model

In figure 3(D), predictions for the single-layered PWS model are shown, where $R_1 = R_3$, which was varied between 0 and 100 μm in steps of 20 μm. As expected (Verkruysse *et al* 1997), large-radius blood vessels (> 20 μm) reduce the influence of wavelength upon vascular injury, consistent with Monte Carlo results from discrete models (Smithies and Butler 1995, Lucassen *et al* 1996). At small vessel radii (< 20 μm) a maximum in Q_3
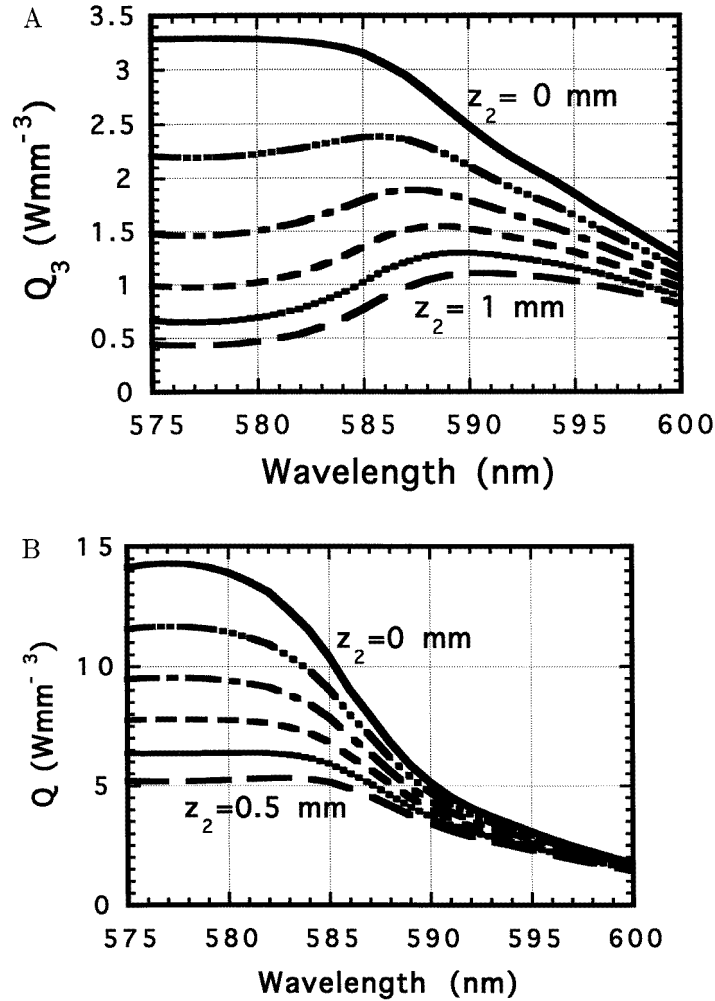
Figure 3. Cross sectional average volumetric heat production in the deepest targeted blood vessel, $Q_3(z_3)$, according to equation (3), normalized to $EA_e = 1$ (W mm^{-2}), for the four models summarized in table 1. (A) The first model, where $z_1 = 0.3$ mm; z_2 is, respectively 0 (top curve), 0.2, 0.4, 0.6, 0.8 and 1 mm (bottom curve). (B) The second model, where $z_1 = 0.15$ mm; z_2 is, respectively, 0 (top curve), 0.1, 0.2, 0.3, 0.4 and 0.5 mm (bottom curve). (C) The third model, where z_1 is, respectively, 0 (top curve), 0.2, 0.4, 0.6, 0.8 and 1 mm (bottom curve). (D) The fourth model, where $R_1 = R_3$, which are respectively, 0 (top curve at $\lambda > 587$ nm), 20, 40, 60, 80 and 100 μm (bottom curve at $\lambda > 583$ nm).

occurs at wavelengths between 585 and 587 nm, consistent with results from homogeneous models (van Gemert *et al* 1995b, Kienle and Hibst 1995).

4. Discussion

Because the homogeneous models lacked correction of the fractional volumetric blood concentration for finite-radius blood vessels, fluence rate distributions used were too strongly attenuated with skin depth, especially for large-radius PWS vessels. The correction factor
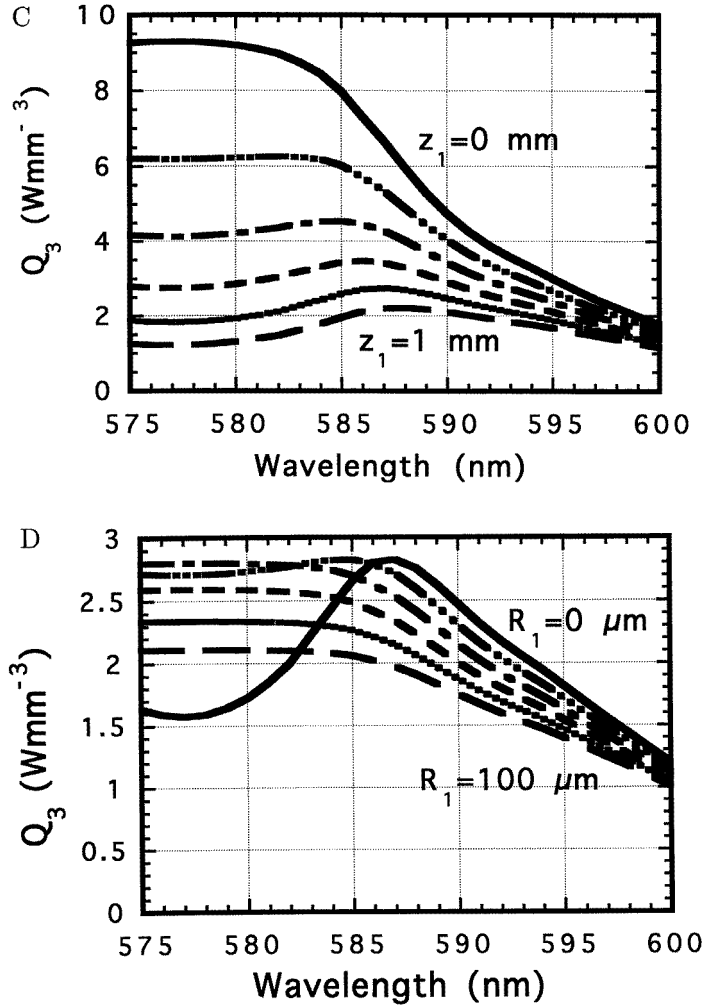
Figure 3. (Continued)

included in the homogeneous model provides results consistent with those obtained from discrete vessel models. This is because the fluence rate distribution, equation (1), depends exponentially on the product $C\mu_{ab}$ in (2). For large-radius vessels, $C\mu_{ab}$ tends to become wavelength independent in the range 577–590 nm; for small-radius vessels $C\mu_{ab} \approx \mu_{ab}$, and hence is strongly wavelength dependent.

Subsequently, the importance of wavelength for PWS laser treatment was reexamined using the correction factor in a homogeneous analytic model of four representative different PWS anatomies. The compound skin model used consists of *two* dermal layers, each of which contains a homogeneous fractional volumetric blood concentration.

The cross sectional average volumetric heat production in the deepest targeted PWS vessel is predicted to have minimal wavelength dependence in the range 577–590 nm when light propagates through a dermal layer composed of large-radius blood vessels. However, maxima occur in Q_3 at wavelengths longer than 577 nm when one of the two dermal layers

contains small-radius vessels and is of sufficient thickness (e.g. > 0.2 mm). Recalling that this case may represent typical PWS anatomy, the results explain Tan's observations of wavelength-dependent depth of vascular injury in pig skin (Tan *et al* 1989a) and in previously untreated as well as treated PWS (Tan *et al* 1990).

Results from the model indicate that 585–587 nm are virtually always excellent wavelengths for treatment in patients with deep PWS vessels. In contrast, maxima in Q_3 occur at 577 nm if the first layer is sufficiently thin (e.g. < 150 μm) and contains relatively small-radius PWS blood vessels (e.g. $R_1 < 12.5$ μm), predicting that 577–580 nm wavelengths are optimal to treat young children with light-coloured PWSs. Although the only available study examining treatment efficacy of children with light PWSs is with 577 nm wavelength (Tan *et al* 1989b), subsequent results reported by Alster and Wilson (1994) and Morelli *et al* (1995) seem to confirm our predictions.

With the exception of superficial lesions, the superiority of laser treatment at 585–587 nm over 577–580 nm wavelengths is therefore predicted. For superficial lesions, 577–580 nm wavelengths are predicted to be more efficient than 585–587 nm to deposit heat in the deepest targeted vessel. From a practical standpoint, however, we expect that in superficial lesions (e.g. $z_3 < 0.65$ mm) 585 nm can produce sufficient volumetric heat in the deepest targeted PWS vessel to achieve selective irreversible vascular injury.

The model presented is simple and analytically solvable, and allows assessment of the effect of wavelength, fractional volumetric blood concentration, blood vessel radii, and dermal anatomy on the volumetric heat production in the deepest targeted PWS vessel. Correct estimates of the light distribution at deeper positions in the skin are obtained, but the increase in fluence rate close to the air–tissue interface may be underestimated when wavelength increases from 577 to 600 nm. As the present analysis neglects this effect, taking A_e in (1) as wavelength independent, the model may underestimate the extent of wavelength-dependent effects occurring during laser treatment. An example may be the observed (0.72 mm) and predicted (0.95 mm) depth of vascular injury at 577 nm assuming a value of 1.16 mm at 585 nm.

We have sought to define the ideal laser wavelength to achieve selective photothermolysis in PWSs, without explicitly including the effect of pulse duration. Appropriate choice of this parameter is important to ensure heat deposition remains confined to the vessel volume and has been discussed previously (Svaasand *et al* 1995, de Boer *et al* 1996, van Gemert *et al* 1997).

5. Conclusion

Correcting the homogeneous fractional volumetric blood concentration for finite-radius blood vessels and combining this with compound, two-layered dermal homogeneous PWS models, we predict fluence rate distributions equal to those from discrete models, and wavelength-dependent effects consistent with clinical observations by Tan *et al* (1990).

Analysis of the importance of wavelength for PWS laser treatment suggests that the volumetric heat production in the deepest targeted blood vessel can be maximized on an individual patient basis.

The results of the model indicate that 577–580 nm wavelengths are optimal to treat *superficial* lesions, while 585–587 nm are wavelengths of choice for remaining PWS categories. However, absorption of light at 585–587 nm wavelengths is sufficiently high in superficial lesions, so we hypothesize that these wavelengths may be considered adequate for the treatment of any PWS.

Acknowledgments

References

Alster T S and Wilson F 1994 Treatment of port-wine stains with the flashlamp-pumped pulsed dye laser: extended clinical experience in children and adults *Ann. Plast. Surg.* **32** 478–84

Anderson R R and Parrish J A 1981 Microvasculature can be selectively damaged using dye lasers: A basic theory and experimental evidence in human skin *Lasers Surg. Med.* **1** 263–70

Barsky S H, Rosen S, Geer D E and Noe J M 1980 The nature and evolution of port wine stains: a computer assisted study *J. Invest. Dermatol.* **74** 154–7

de Boer J F, Lucassen G W, Verkruysse W and van Gemert M J C 1996 Diameter dependence of the thermolysis of port wine stain blood vessels on the laser pulse length *Lasers Med. Sci.* **11** 177–80

Kienle A and Hibst R 1995 A new optimal wavelength for treatment of port wine stains? *Phys. Med. Biol.* **40** 1559–76

Lucassen G W, Verkruysse W, Keijzer M and van Gemert M J C 1996 Light distributions in a port wine stain model containing multiple cylindrical and curved blood vessels *Lasers Surg. Med.* **18** 345–57

Morelli J G, Weston W L, Huff C and Yohn J J 1995 Initial lesion size as a predictive factor in determining the response of port-wine stains in children treated with the pulsed dye laser *Arch. Pediatr. Adolesc. Med.* **149** 1142–4

Pickering J W and van Gemert M J C 1991 585 nm for the treatment of port wine stains: a possible mechanism *Lasers Surg. Med.* **11** 616–18

Smithies D J and Butler P H 1995 Modelling the distribution of laser light in port-wine stains with the Monte Carlo method *Phys. Med. Biol.* **40** 701–31

Star W M 1995 Diffusion theory of light transport *Optical–Thermal Response of Laser Irradiated Tissue* ed A J Welch and M J C van Gemert (New York: Plenum) ch 6, pp 131–206

Svaasand L O, Fiskerstrand E J, Kopstad G, Norvang L T, Svaasand E K, Nelson J S and Berns M W 1995 Therapeutic response during pulsed laser treatment of port wine stains; dependence on vessel diameter and depth in dermis *Lasers Med. Sci.* **10** 235–43

Tan C Y, Stratham B, Marks R and Payne P A 1982 Skin thickness measurement by pulsed ultrasound: its reproducibility, validation and variability *Br. J. Dermatol.* **106** 657–67

Tan O T, Morrison P and Kurban A K 1990 585 nm for the treatment of port-wine stains *Plast. Reconstr. Surg.* **86** 1112–17

Tan O T, Murray S and Kurban A K 1989a Action spectrum of vascular specific injury using pulsed irradiation *J. Invest. Dermatol.* **92** 868–71

Tan O T, Sherwood K and Gilchrest B A 1989b Treatment of children with port-wine stains using the flashlamp-pulsed tunable dye laser *N. Engl. J. Med.* **320** 416–21

van Gemert M J C and Hulsbergen Henning J P 1981 A model approach to laser coagulation of dermal vascular lesions *Arch. Dermatol. Res.* **270** 429–39

van Gemert M J C, Nelson J S, Milner T E, Smithies D J, Verkruysse W, de Boer J F, Lucassen G W, Goodman D M, Tanenbaum B S, Norvang L T and Svaasand L O 1997 Non-invasive determination of port wine stain anatomy and physiology for optimal laser treatment strategies *Phys. Med. Biol.* at press

van Gemert M J C, Welch A J, Pickering J W and Tan O T 1995a Laser treatment of port wine stains *Optical–Thermal Response of Laser Irradiated Tissue* ed A J Welch and M J C van Gemert (New York: Plenum) ch 23, pp 789–829

van Gemert M J C, Welch A J, Pickering J W, Tan O T and Gijsbers G H M 1995b Wavelengths for laser treatment of port wine stains and telangiectasia *Lasers Surg. Med.* **16** 147–55

Verkruysse W, Lucassen G W, de Boer J F, Smithies D J, Nelson J S and van Gemert M J C 1997 Modelling light distribution of homogeneous versus discrete absorbers in laser irradiated turbid media *Phys. Med. Biol.* at press

Verkruysse W, Pickering J W, Beek J F, Keijzer M and van Gemert M J C 1993 Modelling the effect of wavelength on pulsed dye laser treatment of port wine stains *Appl. Opt.* **32** 393–8